Cooperative Terrain-Aided Navigation of AUVs using Particle Filters

Luca Baglivo [1], Pramod Kumar [2]

31 March 2013

Draft

Technical Report
MORPH-CTAN-13-01

Laboratory of Robotics and Systems in Engineering and Science (LARSyS)
Dynamical Systems and Ocean Robotics (DSOR) Group
Instituto Superior Técnico (IST) IST,Torre Norte, Piso 8 Av. Rovisco Pais, 1 1049-001, Lisbon, Portugal

[1]The author benefits of a research grant from the FCT, Portugal, reference 'SFRH/BPD/87974/2012
[2]Supervisors: Prof. António Pascoal

Contents

Abstract

This report is in the context of non-conventional geophysical based navigation of Underwater Autonomous Vehicles (UAVs). Here is proposed a particle filter algorithm that can be applied to the case of Terrain-Aided Navigation (TAN) when distributed sensing over two or more (communicating) vehicles is available. The remote sensing information is conveyed in a centralized navigation filter for the estimation of one vehicle (*opportunistic*) or more (*cooperative*) vehicles position by using the information gained by the group of vehicles. The measurements used are the altitudes with respect to the seabed and the ranges between UAVs. The map of the seabed is known.
The case of the update step of a static two-vehicles network is analysed with a proposed solution and its implementation. An alternative to the standard approach for *pdf* marginalization is proposed. After setting this kernel, some details of the full filter for the dynamic state estimation follow. Premilinary experimental results are presented, using the Medusas AUV of the DSOR group at Expo area in Lisbon. Open issues and considerations are collected as a basis of further discussion.

Introduction

The Terrain-Aided Navigation problem consists in using bathymetric measurements acquired along the trajectory of an AUV to estimate the vehicle's position and, eventually, the vector of velocity measurement bias (or gyro measurement bias like in [1]). This is a nonlinear problem due to the nonlinear nature of the measurement model. This model relates measurements provided by the acoustic sensors installed on-board with the three-dimensional position and the orientation of the vehicle relative to the sea-bottom represented with a map. For the single vehicle TAN, a set of up-to-date solutions can be found in [2, 1] and the references therein. In [2] a novel complementary filtering technique is presented, it also implements the PPF version presented in [3]. Attention must be payed to the work in [1, 4] where interesting concepts are analysed, e.g. the integration of the noise of the map and of its interpulation is taken into account. A model of the correlation betweem map noise and measurement noise thorughout the vehicle trajectory is included in [4]. A best selection of this techniques for single TAN can be implemented and integrated into the cooperative TAN algorithm here presented.

It is easy to understand that TAN intrinsically suffers from the problem of flat and featureless terrain. To mitigate the fall of performances, in [4] the authors propose a more robust adaptive strategy which adjust the filter variance according to the estimated terrain information. To cope with these TAN limitations and improve the general robustness of TAN, as stated in section 1, we aim at taking advantage of a AUVs network sensing strategy. Intuitively, each AUV can benefit from the measurements obtained by the other AUVs. The estimation of the state of the single AUV is improved by incorporating all the available information in a filter which in the limit results in a fully decentralised approach. This concept has been extensively exploited in Field Robotics to achieve what is called *cooperative* or *collaborative* navigation [5, 6, 7, 8].

Chapter 1

Problem formulation

The problem of what we call *opportunistic* navigation is built starting from the one already stated in [2] and detailed in [9], and extended with a network sensing capability, where the sensor nodes are not physically but logically linked as in the MORPH/FP7/EU project.

1.1 System models

For simplicity of analysis we assume that the vehicle is leveled horizontally and stabilized in roll and pitch, i.e. $\phi = \theta = 0$ so that the angular velocity yaw rate is given by $r = \dot{\psi}$. The velocity vector of the current is considered constant or varying very slowly in time. Without loss of generality, we assume that the AUV maintains constant depth (z) which can be measured with high accuracy by using a pressure cell.
From now on we treat z as an input, not as a state variable, thus reducing the dimension of the state vector; this is crucial to the performance of the Particle Filter estimator used in [10]. Thus, the position estimation is reduced to a 2-D estimation problem. The body $\{B\}$ and inertial reference frame $\{I\}$ are also considered in 2-D. See Appendix A of [10] for a full derivation of the 3-D continuous-time model and its discrete-time counterpart. For TAN of a single vehicle, the continuous-time design model in 2D is given by

$$ {}^{I}\mathbf{V} = \mathfrak{R}(\psi)\,{}^{B}\mathbf{V}_{SB}, \tag{1.1} $$

$$ \dot{\mathbf{p}} = {}^{I}\mathbf{V} + \xi_v \tag{1.2} $$

where $\mathbf{p} = [x, y]^T$ is the position of the vehicle, $\mathbf{V}_{SB} = [v_u, v_v]^T$ is the linear velocity relative to the sea bottom expressed in $\{B\}$. The rotation matrix $\mathfrak{R}$ is parametrized by ψ. ${}^{I}\mathbf{V} = [v_x,\, v_y]^T$ is velocity of the AUV expressed in $\{I\}$. In the

above, ξ_v is process noise. The heading angle ψ, the velocity vector V, and yaw rate r are used as inputs to the model. In the 2-D formulation that we will use henceforth the state vector is $\mathbf{x} = [x, y]^T$ and the input vector is $\mathbf{u} = [v_x, v_y, z]^T$. The discrete-time process and measurement models for the $2D$ TAN problem can now be written as

$$\mathbf{x}_{k+1} = F\mathbf{x}_k + G_u\mathbf{u}_k + \zeta_k \tag{1.3}$$

$$\mathbf{y}_k = h(\mathbf{x}_k) + \eta_k(\mathbf{p}_k), \tag{1.4}$$

where $h(\mathbf{x}_k)$ represents the altitude of the vehicle above the terrain, ζ_k is process noise and η_k is measurement noise; the latter is a function of position $\mathbf{p}_k$. In the above, F and G_u are matrices of appropriate sizes that depend on the sampling period T and G_u is a function of the input u . Notice that

$$h(\mathbf{x}_k) = m(x, y) - z \tag{1.5}$$

where $m(x, y)$ is the terrain elevation (bathymetric) map measured from the surface and z is the depth of operation of the AUV. Notice also that $\eta_k(\mathbf{p})$ captures both measurement noise and map errors, including those that arise in the process of smoothing that same map. For our purposes, $\eta_k(\mathbf{p})$ will be modeled as Gaussian white noise. We note, however, that the parameters of the gaussian distribution that models the sonar range error may change, depending on the acoustic properties of the sea-bottom material. A more realistic model is proposed in [11] by using a sum of gaussians. See also the uncertainty model derived in [10] that allows the parametrization of sea-bottom properties, including bottom surface roughness and reflectance parameters.
For the case of more AUVs we suffix the number to the states in order to identify the AUVs, for example position vector of AUV1 is represented as $\mathbf{p}^1 = [x^1, y^1]^T$. The observation models, in the case of more than one AUV, will be changed accordingly in the following sections.

The problem is set as follows:

Given the kinematic models of two underwater vehicles AUV1 and AUV2, a bathymetric map of the area of interest, and measurements of ranges and velocity obtained by the two vehicles with respect to the seabed, estimate the position of AUV1 relative to an inertial frame using: its own measurements, the inter-range measurements between AUV1 and AUV2 and the communicated measurements obtained by AUV2.

Therefore, we want to estimate the position of AUV1 with respect to an inertial frame. The rationale of the former problem formulation is rooted in the system configuration features. We focus on the estimation of AUV1 aided also by

the measurements provided by AUV2 because we assume that AUV2, due to its reduced sensor suites (*and navigation capability*), is limited in estimating its position but can increase the robustness of AUV1 estimation. For instance, AUV2 can navigate using a Range-Only-Formation control strategy within a group of vehicles. Furthermore, in the cooperative perspective, AUV1, having a more accurate sensor suite and centralized sensing information, can provide a better estimation of AUV2 position.

Chapter 2

The opportunistic navigation algorithm

2.1 Static Bayesian opportunistic update

We aim at defining the key probabilistic tool for fusing information at each communication step between the two vehicles, that is the probabilistic update step of a Bayesian filter for the estimation of AUV1 position when AUV2 observations are also available. A similar approach (also implemented in the form of a distributed particle filter, check Section 2.2) can be find in [12] where they assume that all robots have all the same sensor suites and each robot can do range-and-bearing measurements to detect another robot. Instead, we assume heterogeneous robots with different capabilities and a range-only detection model. We firstly assume that the two vehicles are static, therefore their states are time independent, and that AUV2 has communicated its measurements set to AUV1. The resulting observation set for AUV1 is $\mathbf{Y}^1 = \{\mathbf{a}^1, \rho^{12}, \mathbf{a}^2\}$, where the first two elements are respectively the set of simultaneous ranges to the seabed obtained by AUV1 and AUV2, and $\rho^{12} = ||\mathbf{p}^{12}|| = ||\mathbf{p}^2 - \mathbf{p}^1||$ is the inter-range between the two vehicles. Given the set of measurements $\mathbf{Y}^1$, we want to compute the belief over $\mathbf{x}^1$, being $\mathbf{x}^1$ the discrete-time representation of $\mathbf{p}^1$. The posterior (*pst*) *pdf* of $\mathbf{x}^1$ is proportional to the product of the measurements likelihood (*llh*) and the prior (*prr*), as follows from Bayes theorem:

$$p_{pst}(\mathbf{x}^1|\mathbf{Y}^1) \propto p_{llh}(\mathbf{Y}^1|\mathbf{x}^1)p_{prr}(\mathbf{x}^1) \tag{2.1}$$

From now on, for the sake of notation simplicity we will omit the label of each *pdf* , denoting all of them as $p(\cdot)$. We get to the factorization of the likelihood density by means of the chain rule and the assumption of conditional independence of the measurements given the state:

$$
\begin{aligned}
p(\mathbf{Y}^1|\mathbf{x}^1) &= p(\mathbf{a}^1, \rho^{12,\mathbf{a}^2}|\mathbf{x}^1) \\
&= p(\mathbf{a}^1|\mathbf{a}^2, \rho^{12}, \mathbf{x}^1)\, p(\mathbf{a}^2, \rho^{12}|\mathbf{x}^1) \\
&= p(\mathbf{a}^1|\mathbf{x}^1)\, p(\mathbf{a}^2, \rho^{12}|\mathbf{x}^1) \\
&= p(\mathbf{a}^1|\mathbf{x}^1)\, p(\mathbf{a}^2|\rho^{12}, \mathbf{x}^1)\, p(\rho^{12}|\mathbf{x}^1)
\end{aligned}
\tag{2.2}
$$

If we have *no prior knowledge* of the relation between $\mathbf{p}^1$ and $\mathbf{p}^2$, we can discard the factor $p(\rho^{12}|\mathbf{x}^1)$ as a uniform density (otherwise, e.g. we could include the information from a range-only formation control that can give a prediction of the behaviour of the other vehicle). The full measurements likelihood can be expressed as:

$$
p(\mathbf{Y}^1|\mathbf{x}^1) \propto p(\mathbf{a}^1|\mathbf{x}^1)\, p(\mathbf{a}^2|\rho^{12}, \mathbf{x}^1) \tag{2.3}
$$

Substituting Eq. 2.3 in Eq. 2.1 we get:

$$
p(\mathbf{x}^1|\mathbf{Y}^1) \propto p(\mathbf{x}^1)\, p(\mathbf{a}^1|\mathbf{x}^1)\, p(\mathbf{a}^2|\rho^{12}, \mathbf{x}^1) \tag{2.4}
$$

Since the set of range measurements of AUV2 with respect to the seabed is dependent on the vehicle position $\mathbf{x}^2$, we marginalize the last factor in Eq. 2.4 as follows:

$$
\begin{aligned}
p(\mathbf{a}^2|\rho^{12}, \mathbf{x}^1) &= \int p(\mathbf{a}^2, \mathbf{x}^2|\rho^{12}, \mathbf{x}^1) d\mathbf{x}^2 \\
&= \int p(\mathbf{a}^2|\mathbf{x}^2, \rho^{12}, \mathbf{x}^1)\, p(\mathbf{x}^2|\rho^{12}, \mathbf{x}^1) d\mathbf{x}^2 \\
&= \int p(\mathbf{a}^2|\mathbf{x}^2)\, p(\mathbf{x}^2|\rho^{12}, \mathbf{x}^1) d\mathbf{x}^2
\end{aligned}
\tag{2.5}
$$

In the above derivation some conditional independence assumptions have been made and consequently the relative stochastic variables dropped. Applying the Bayes rule to the last factor in the integral of Eq. 2.5 we obtain:

$$
\begin{aligned}
p(\mathbf{x}^2|\rho^{12}, \mathbf{x}^1) &= p(\mathbf{x}^1|\rho^{12}, \mathbf{x}^2)\, p(\rho^{12}|\mathbf{x}^2)\, p(\mathbf{x}^2) \\
&\propto p(\mathbf{x}^1|\rho^{12}, \mathbf{x}^2)\, p(\mathbf{x}^2)
\end{aligned}
\tag{2.6}
$$

Again, we made the assumption of *no knowledge* about the inter-range ρ^{12} given a position $\mathbf{x}^2$. Substituting Eq. 2.6 in Eq. 2.5 we get:

$$
\begin{aligned}
p(\mathbf{a}^2|\rho^{12},\mathbf{x}^1) &= \int \underbrace{p(\mathbf{a}^2|\mathbf{x}^2)\,p(\mathbf{x}^2)}_{\text{Bayes}}\, p(\mathbf{x}^1|\rho^{12},\mathbf{x}^2)\,d\mathbf{x}^2 \\
&= \int p(\mathbf{x}^2|\mathbf{a}^2)\,p(\mathbf{x}^1|\rho^{12},\mathbf{x}^2)\,d\mathbf{x}^2
\end{aligned}
\tag{2.7}
$$

Finally, substituting Eq. 2.7 in Eq. 2.4 we obtain:

$$
\begin{aligned}
p(\mathbf{x}^1|\mathbf{Y}^1) &\propto \underbrace{p(\mathbf{x}^1)\,p(\mathbf{a}^1|\mathbf{x}^1)}_{\text{Bayes}} \int p(\mathbf{x}^2|\mathbf{a}^2)\,p(\mathbf{x}^1|\rho^{12},\mathbf{x}^2)\,d\mathbf{x}^2 \\
&= p(\mathbf{x}^1|\mathbf{a}^1) \int p(\mathbf{x}^2|\mathbf{a}^2)\ \underbrace{p(\mathbf{x}^1|\rho^{12},\mathbf{x}^2)}_{\text{detection model}}\ d\mathbf{x}^2
\end{aligned}
\tag{2.8}
$$

The last equation states that, provided that we have the posteriors of $\mathbf{x}^1$ and $\mathbf{x}^2$ given their respective range measurements with respect to the seabed, we can update the distribution of the state $\mathbf{x}^1$ by integrating the detection model of $\mathbf{x}^1$, *weigthed* with the posterior of $\mathbf{x}^2$, over all possible $\mathbf{x}^2$ and fuse the result with the posterior of $\mathbf{x}^1$. After updating the state of $\mathbf{x}^1$, vice versa, we can also update the posterior of $\mathbf{x}^2$ in the reciprocal way. A similar collaborative approach has been proposed by [13] and recently applied with some modifications in [12].

The standard approach described above has shown to be not best suited for a particle filter implementation as a solution to opportunistic TAN. The integral term, in Eq. 2.8 coming from the marginalization phase, is not suitable when a *pdf* factor, which depends on the state over which the marginalization is done, is strongly multi-modal, as could be in this case for the posterior $p(\mathbf{x}^2|\mathbf{a}^2)$. It has been found, both in simulation and experimental analyses, that this approach can lead to the opportunistic particle filter divergence. As it will be illustrated, the cause is related to the representation, by discretization with particles, of the probability density of the marginalized distribution. When the probabilistic distribution of the state of AUV2 is multimodal or is strongly non-Gaussian, e.g. because of the characteristics of the terrain, the resulting marginalized distribution of AUV1 state can be highly peaked in some regions when the hypotheses are (virtually) concurrent. If the number of particles is not enough high to represent these density peaks, the filter doesn't work properly. Instead of increasing the number of particles, a modification to the marginalized distribution has shown to be promising. Instead of computing the integral, a maximization approach is here used and proposed. The resulting equation is:

$$
p(\mathbf{x}^1) = p(\mathbf{a}^1|\mathbf{x}^1) \max_{\mathbf{x}^2 \epsilon X^2} \left(p(\mathbf{x}^2|\mathbf{a}^2)\,p(\mathbf{x}^1|\rho^{12},\mathbf{x}^2) \right) \tag{2.9}
$$

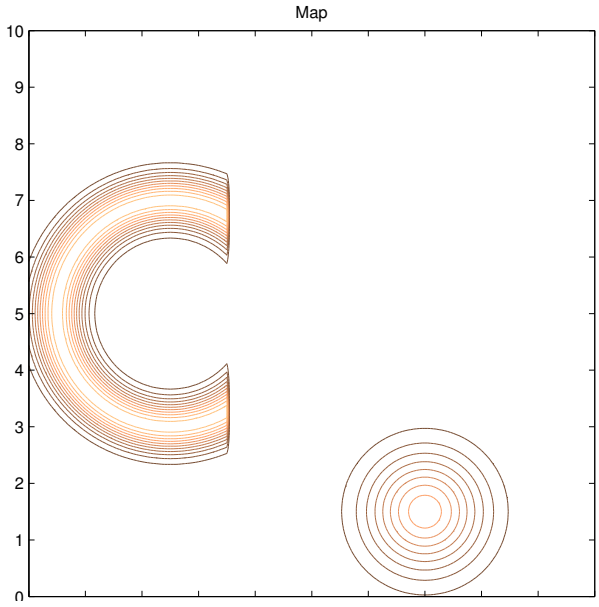

Figure 2.1: Contour lines of the map with a C-shaped volcano on the left and a hill on the bottom right

The difference between the two approaches (Eq. 2.8 vs Eq. 2.9) is illustrated with the example in Fig. 2.2 and Fig. 2.3. In this example the synthetic map consists of a C-shaped volcano and a smaller hill (Fig. 2.1), the rest of the map being flat. AUV2 is measuring an altitude $\mathbf{a}^2$ which corresponds to the top edge elevation of the volcano. The range between AUV1 and AUV2, ρ^{12}, is assumed equal to the range of that circular top edge. The belief of AUV2 is the same in the two cases and is given in the pictures on the left of Fig. 2.2 and Fig. 2.3. Assuming no prior and no $\mathbf{a}^1$ altitude is available for AUV1, the belief of AUV1 $p(\mathbf{x}^1) = p(\mathbf{x}^1|\mathbf{a}^2, \rho^{12})$ is represented in the pictures on the right of Fig. 2.2 and Fig. 2.3 for the two different approaches. It is evident that the standard approach (Eq. 2.8) leads to a belief of AUV1 with high density in the inner area of the volcano. This is due to the summing effect of all the high-probability positions of AUV2 distributed uniformly on top the circular edge. On the other hand, the approach using Eq. 2.9 turns out in a flatter belief of AUV1, as it would be expected, because no prior hypothesis have been done for AUV1: the inner and the outer areas around the volcano are expected to have similar probability values. This result is granted by the modified belief obtained from Eq. 2.9 (picture on the right in Fig. 2.3).

Considerations: an issue could be the double counting information and therefore overconfidence when the reciprocal updating is 'too' frequent, IF we include a filter

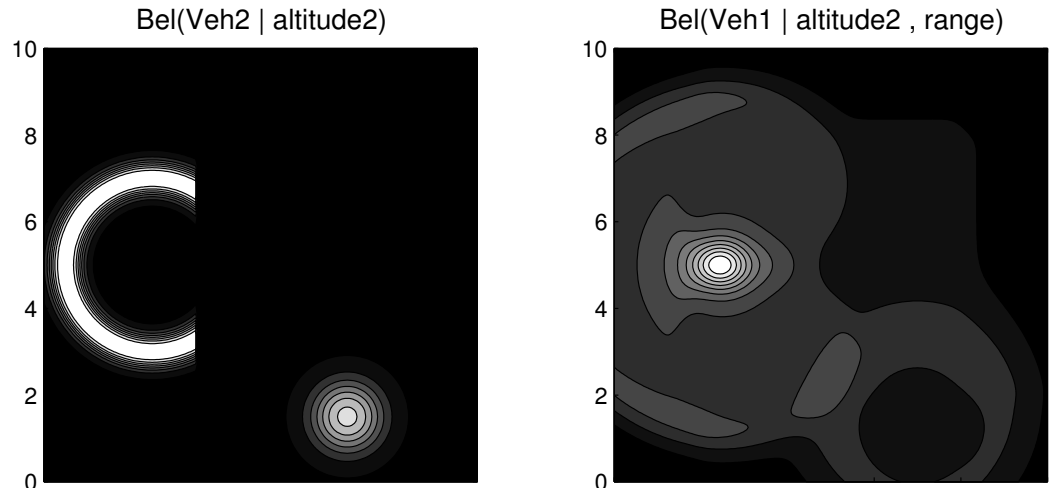

Figure 2.2: Left: likelihood of AUV2 given its altitutude measurements $\mathbf{a}^2$ and a uniform prior over the map. Right: Belief of AUV1 position using only altitude and range obtained from AUV2 and uniform prior over the map, application of Eq. 2.8

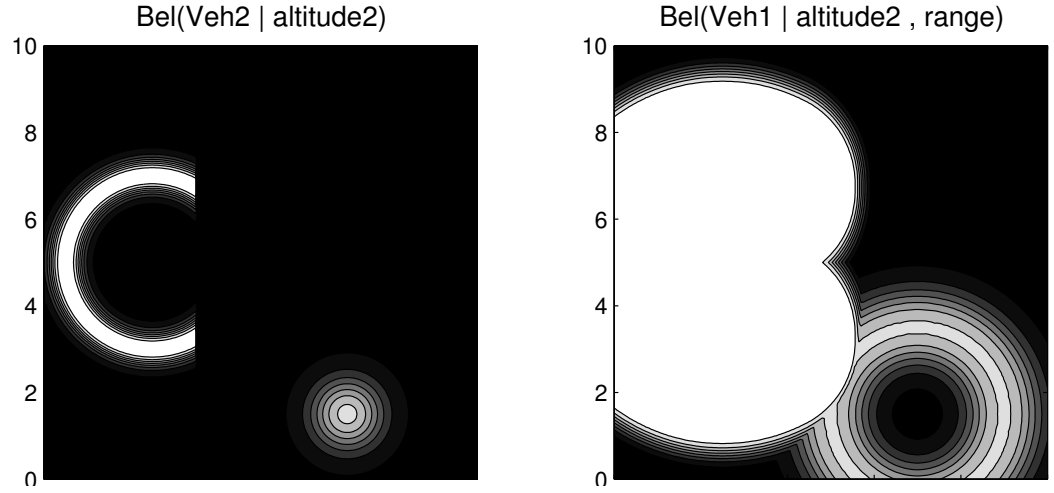

Figure 2.3: Left: likelihood of AUV2 given its altitutude measurements $\mathbf{a}^2$ and a uniform prior over the map. Right: Belief of AUV1 position using only altitude and range obtained from AUV2 and uniform prior over the map, application of Eq. 2.9

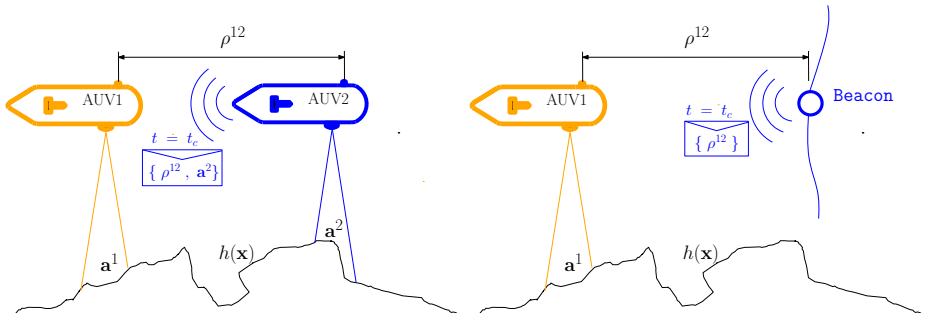

Figure 2.4: Communication frameworks in the case of the proper opportunistic TAN with 2 vehicles (left) and of Unknown Single Beacon playing the role of AUV2 (right)

also for AUV2 position estimation in the opportunistic filter. On the one hand, if we reset the prior of $\mathbf{x}^2$ *in the opportunistic filter for* $\mathbf{x}^1$ *this issue doesn't hold, on the other hand if we run a filter for* $\mathbf{x}^2$ *the overconfidency problem is mitigated in the case AUV2 always move and is not still. In [12] they propose to solve the problem with a naive reciprocal sampling by substituting part of the particles with those coming from the detection model, unfortunately it is particularly suited for range and bearing detections and not only-range detections (i.e. for fully observable states).*
Other authors propose to introduce a discounting exponent which 'flatten' the pdf to reduce overconfidence [14].
Another problem is eventually given by outliers in inter-range measurements: a wrong information can bias the estimation and bring to filter divergence. An outlier range measurement which is strongly unlikely to belong to its assumed pdf , could make the particle filter for $\mathbf{x}^1$ *reset since all its weights will be set to near-zero values.*

2.2 Opportunistic TAN implementation with particle filter

We propose a particle filter setup to implement the Bayesian update presented in section 2.1, in its *opportunistic* form and with the modification proposed for the marginalization step (Eq. 2.9).
We recall that we are focusing on the estimation of AUV1 state $\mathbf{x}^1$ using also the measurements communicated by AUV2 (see Fig. 2.4).

The observation vector $\mathbf{y}^1$ is the set of simultaneous range measurements to the seabed (e.g. 4 ranges from a DVL sensor), $\mathbf{y}^1 = \mathbf{a}^1$. The subscript c (check Fig. 2.4) is related to the communication event: at each time instant t_c when

AUV2 communicates its data to AUV1, the inter-range ρ^{12} and the altitude, $\mathbf{a}^2$, of AUV2 with respect to the seabed, are also available ($\mathbf{y}^1 = [\mathbf{a}^1, \rho^{12}, \mathbf{a}^2]$). The noise component relative to ρ^{12} is assumed Gaussian with variance σ_ρ^2. It is worth noticing that if we substitute the moving AUV2 with a fixed single beacon (Unknown Single Beacon Navigation, USBN) which position is unknown, the implementation structure will remain the same, the only difference being the process noise modelling for the second agent and the absence of $\mathbf{a}^2$ measurements.
The *communication delay* is assumed to be zero in the scope of the filter design, nevertheless it should be taken into account.

2.2.1 Opportunistic update step

In the particle filter setup, the *pdf* of the position $\mathbf{p^l}(\mathbf{t})$ of AUV-l is approximated by the set of particles $X_k^l = \{\mathbf{x}_k^{l,i}\}_{i=1}^N$ and its associated set of weights $\Omega_k^l = \{\omega_k^{i,l}\}_{i=1}^N$.

Here is reported a particle filter implementation algorithm of the opportunistic update step described in section 2.1 and resulting in Eq. 2.8, with the important modification of Eq. 2.9.

The prior for $\mathbf{x}^2$ is represented either by a uniform distribution (if we reset to complete ingnorance the information about this state) or by a prediction computed within the AUV1 navigation module. In this implementation, the particle set for AUV2 has been replaced with a grid placed on the map according to the inter-range data and its uncertainty, as explained in the followings.

Finally, the posterior $p(\mathbf{x}^1|\mathbf{y}^1)$ is represented by the N weights $\omega^{1,j}$ obtained by trasforming Eq 2.9 in its corresponding discrete version for the particle filter.

$$\omega_k^{1,j} = \max_{\mathbf{x}_k^{2,i} \epsilon X_k^2} \left(\omega_k^{2,i} \; exp\left(-\frac{1}{2} \left(\frac{\left\| \mathbf{x}_k^{2,i} - \mathbf{x}_k^{1,j} \right\| - \rho_k^{12}}{\sigma_{\rho_k^{12}}} \right)^2 \right) \right) \qquad j = 1, .., N \quad (2.10)$$

Where: $\omega_k^{2,i}$ are the weights that represent the likelihood $p(\mathbf{x}^2|\mathbf{a}^2)$ and $\omega^{1,j}$ represents the posterior of $\mathbf{x}^1$ after the opportunistic update, i.e. the weights computed after the prediction, the self-update, and the opportunistic steps using respectively the motion model, the likelihood of measurement $\mathbf{a}^1$ and the detection model from $\mathbf{x}^2$ with measurement ρ^{12} (exponential term in Equation 2.10).

Using the synthetic map of Fig. 2.1, a simulation of trajectory estimation for AUV1 has been run by means of the particle filter implementation above described, also compared with the standard marginalization (*sum* instead of *max* in Equation 2.10). AUV1 and AUV2 have linear parallel trajectories, AUV2 passes over the top edge of the C-shaped volcano and the range ρ^{12} is equal to the inner radius of the top circular edge. The results are showed in Figure 2.5 and 2.6. The

particles distribution reflects the expected hypotheses as in Figure 2.2 and 2.3: in the standard marginalization approach (left column of frames) the particles tend to concentrate in the inner part of the volcano even if the true position is in the lower outer area. Using not enough particles (500 in the example) lead to particles impoverishment and then filter divergence. In the likelihood maximization approach (right column of frames), instead, 500 particles are enough to keep the filter consistency.

Particular attention must be paid to the calculation of the maximum in Equation 2.10 that could be computation demanding. The same problem would be faced with the calculation of the integral in Equation 2.8 in its particle filter implementation. The domain required for the calculation would be the whole map. In the implementation here used the space support for the maximization is reduced to a smaller grid. This grid at step k is built using the range measurement ρ_k^{12}. This implemetation has some similarity, in the continous probability distributions case, to the non linear filtering approaches using the output injection method [15]. The grid is made of subgrids, each one built around each particle $\mathbf{x}_k^{1,j}$. The subgrid is ring-shaped with a width corresponding to an assigned confidence interval of the detection model (e.g. $\pm 3\sigma_{\rho_k^{12}}$).

2.2.2 Experimental results

A preliminary experimental test has been done at the Expo area in Lisbon using the Medusa AUV vehicles of LaRSys/DSOR. (Figure 2.7).

Two vehicles have been used in this test, nevertheless a third vehicle could be used as a second information source for the opportunistic vehicle. The measured map of the area is reported in Figure 2.8. The performed trajectories are shown in figure 2.9. The application of standard TAN filter performed by a single vehicle and its Opportunistic version, both computed off-line, is illustrated in Figure 2.10. Even though there are many symmetries in the map, the likelihood maximization approach is able to keep filter convergence and show improvements in the estimation with respect to the single TAN filter. The standard marginalization approach has diverged with the same number of particles.

2.3 The Cramér-Rao lower bound (CRLB)

For a cooperative terrain–aided navigation system, the observation model is given by,

$$\mathbf{y}_k = [h_1(\mathbf{x}_k) \quad h_2(\mathbf{x}_k) \quad h_3(\mathbf{x}_k)]^T + \eta_k(\mathbf{p}_k), \tag{2.11}$$

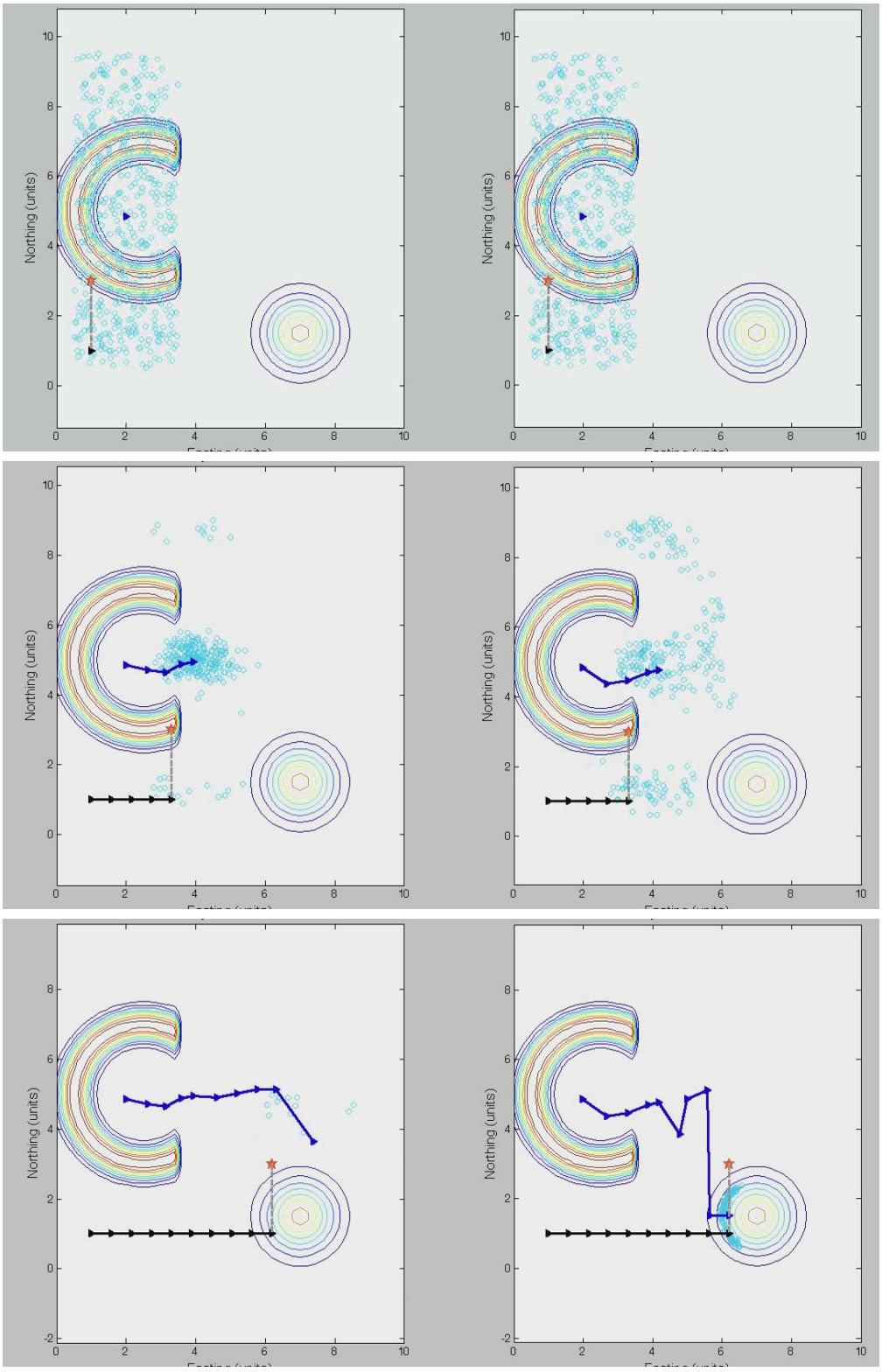

Figure 2.5: Simulation of the Opportunistic TAN comparing the standard marginalization (left column) and the proposed approach with likelihood maximization (right column). SIR particle filter is used with **500 particles**. Black: the true trajectory of AUV1; blue: the estimated trajectory of AUV1; red star: the true AUV2 position.

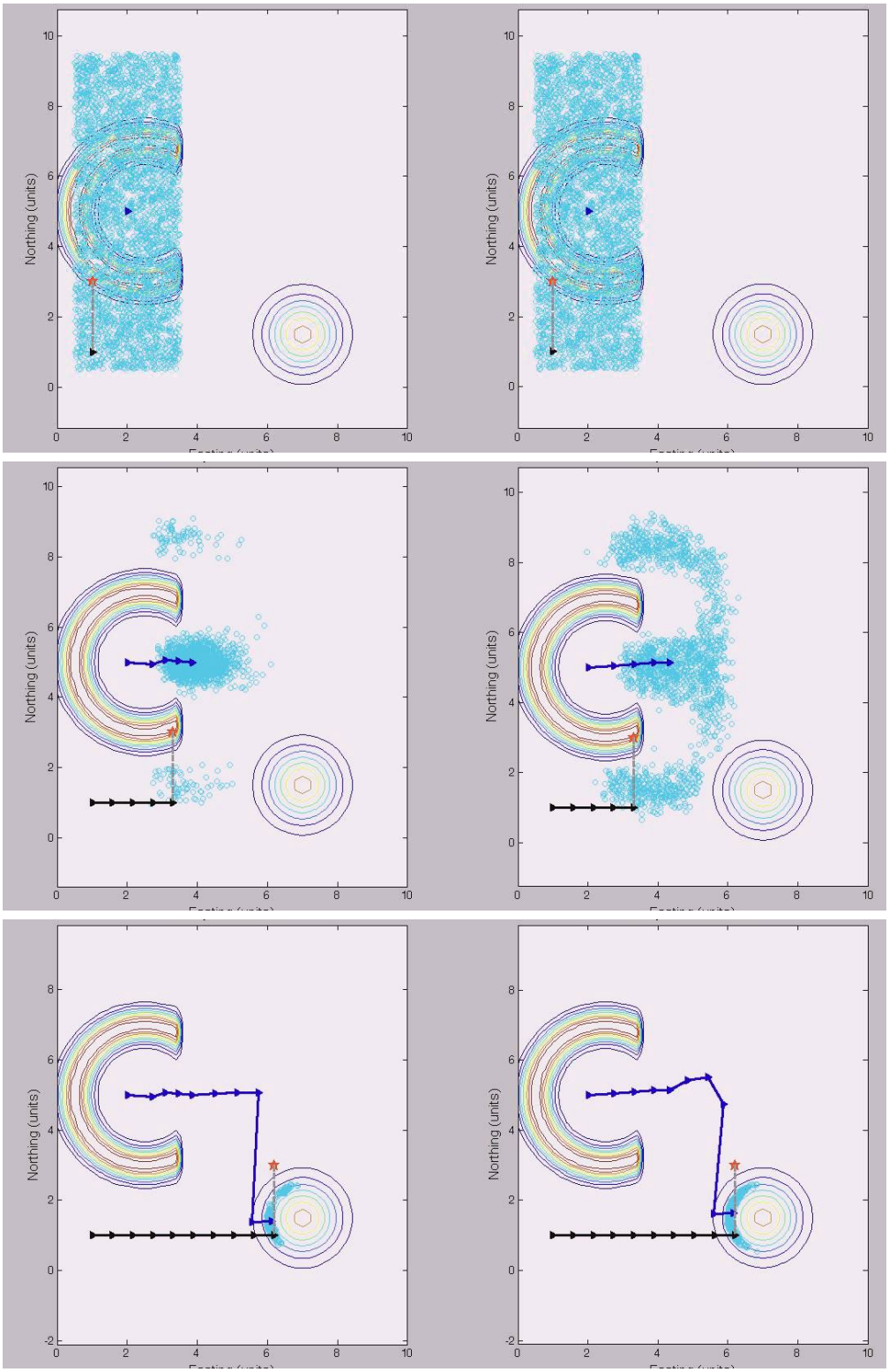

Figure 2.6: As in Figure 2.5 but using **3000 particles**

Figure 2.7: The Medusas vehicles of the Laboratory of Robotics and Systems in Engineering and Science (LARSyS), Dynamical Systems and Ocean Robotics (DSOR) Group, Instituto Superior Técnico (IST), Lisbon.

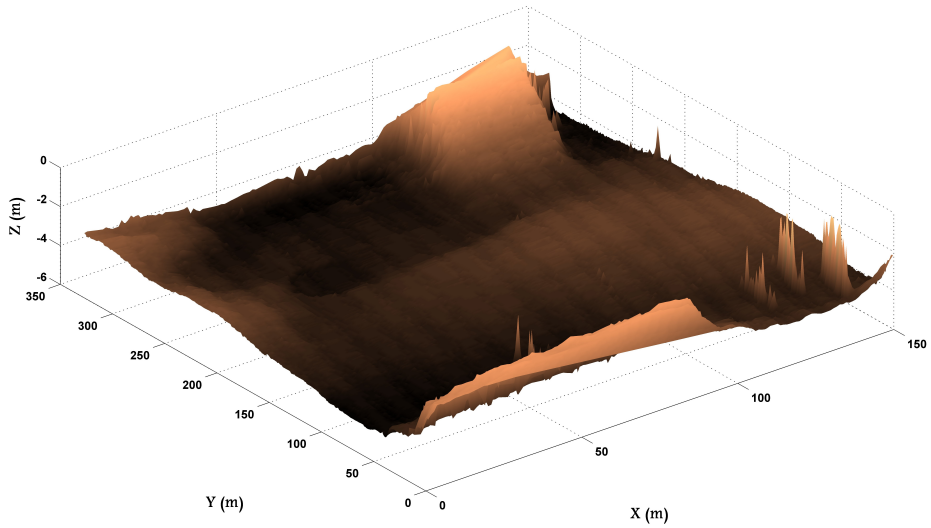

Figure 2.8: Measured map used for the TAN filters.

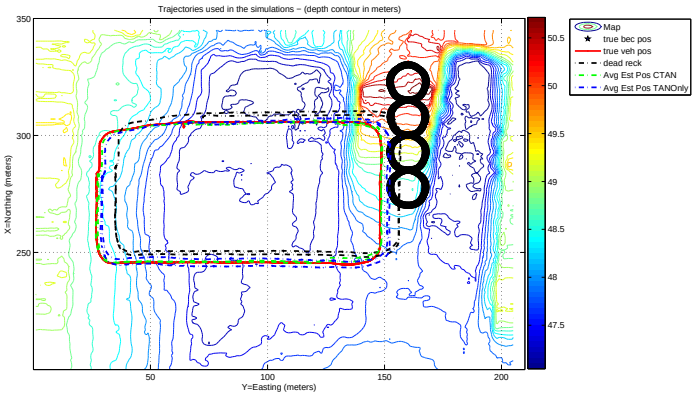

Figure 2.9: Trajectories of the two AUVs Medusas and their estimation with single TAN and Opportunistic TAN

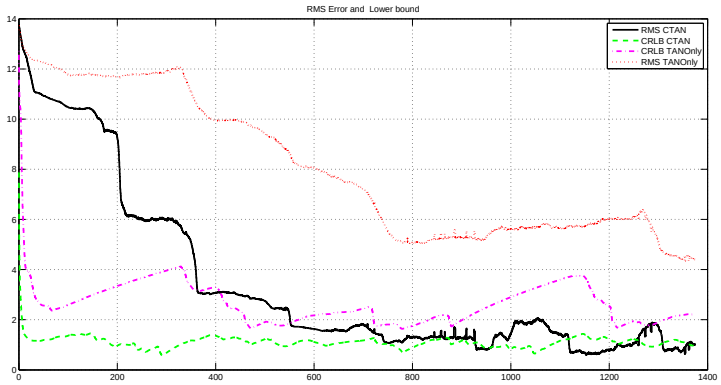

Figure 2.10: RMS error of the trajectory estimation, comparison over off-line runs using the single and Opportunistic TAN, 50 runs.

where $h_1(\cdot)$ is a nonlinear function that represents the measurement model of the echo-sounder (altimeter) installed in AUV1. This model embeds the map of the terrain that has no particular structure. The model for the range measurements relative to the transponder position (position of AUV2) is embodied in the smooth function $h_2(\cdot)$. $h_3(\cdot)$ represents the measurement model of altimeter installed on AUV2. The measurement error is represented by $\eta_k(\mathbf{p}_k) = [\eta_{1_k}(\mathbf{p}_k), \eta_{2_k}(\mathbf{p}_k), \eta_{3_k}(\mathbf{p}_k)]^T$, where $\eta_{1_k}(\mathbf{p}_k)$ and $\eta_{3_k}(\mathbf{p}_k)$ models the errors in the echo-sounder measurements of AUV1 and AUV2 respectively, while $\eta_{1_k}(\mathbf{p}_k)$ models the errors in the measurements of the ranges between the the two vehicles; see Chapter 4 of [10] for more details on the sonar model. The noise signals in the model are assumed to be mutually independent and white, with distributions

$$\zeta_k \sim p_{\zeta_k}(\mathbf{x}_k) = \mathcal{N}(0, \mathrm{Q_k}), \text{ and} \tag{2.12}$$

$$\eta_k \sim p_{\eta_k}(\mathbf{x}_k) = \mathcal{N}(0, \mathrm{R_k}), \tag{2.13}$$

where Q_k and R_k are covariance matrices that may depend on the states. In the above, the noises are assumed to be zero mean only for the sake of simplicity in the computation of CRLB. In reality, these noises are not necessarily zero mean; this is true for the case of TAN measurements obtained with a conventional echo-sounder, where the mean value of the measurement error depends on the local terrain gradient ([10]). We now make the following assumptions: the state of the system, $\mathbf{x}_k$ is considered to be a Markov process such that

$$p\left(\mathbf{x}_k\right) = p\left(\mathbf{x}_0\right) \prod_{i=1}^{k} p\left(\mathbf{x}_i | \mathbf{x}_{i-1}\right) \tag{2.14}$$

applies with $p(\mathbf{x}_0)$ denoting the prior distribution for the state at $k = 0$; the observations are conditionally independent given the states, i.e.,

$$p\left(\mathbf{Y}_k | \mathbf{X}_k\right) = \prod_{i=1}^{k} p\left(\mathbf{y}_i | \mathbf{x}_i\right) \tag{2.15}$$

where $\mathbf{X}_k$ represents the sequence of states $\mathbf{x}_0, \mathbf{x}_1, ..., \mathbf{x}_k$ and $\mathbf{Y}_k$ represents the sequence of observations $\mathbf{y}_1, ..., \mathbf{y}_k$. The prior distribution of position is

$$\mathbf{x}_0 \sim p_0(\mathbf{x}_0) = \mathcal{N}(\bar{\mathbf{x}}_0, \mathrm{P}_0).$$

Given the assumptions on the noise, the prior distribution for $\mathbf{X}_k$ is

$$p(\mathbf{X}_k) = p(\mathbf{x}_k | X_{k-1}) \quad ... \quad p(\mathbf{x}_1 | \mathbf{x}_0) p(\mathbf{x}_0), \tag{2.16}$$

$$= p(\mathbf{x}_0) \prod_{i=1}^{k} p(\mathbf{x}_i - F\mathbf{x}_{i-1} - G_u u_{i-1}), \tag{2.17}$$

where u_i is the input vector represented in (1.3) that includes the linear velocity and the heading angle. In view of the main assumptions made before, it is straightforward to compute the likelihood function

$$p(\mathbf{Y}_k|\mathbf{X}_k) = \prod_{i=1}^{k} p(\mathbf{y}_i - h(\mathbf{x}_i)). \tag{2.18}$$

Recall now the definition of the Fisher information matrix (FIM) $J(\theta)$ that arises in the estimation of a parameter θ given related observations embodied in a stochastic process ζ ([16]):

$$J(\theta) = -E\left[\frac{\partial}{\partial\theta}\left(\frac{\partial}{\partial\theta}\log p_\zeta(\zeta;\theta)\right)\right] \tag{2.19}$$

In what follows we identify θ and ζ with the extended state $\mathbf{X}_k$ and measurement $\mathbf{Y}_k$, respectively. In order to compute sequentially the information submatrix, we decompose $\mathbf{X}_k = [\mathbf{X}_{k-1}^T, \mathbf{x}_k^T]^T$. Following the formulation introduced in [17] we have

$$J(\mathbf{X}_k) = \begin{bmatrix} A_k & B_k \\ B_k^T & C_k \end{bmatrix} = \tag{2.20}$$

$$\begin{bmatrix} E\left[-\Delta_{\mathbf{X}_{k-1}}^{\mathbf{X}_{k-1}}\log p(\mathbf{X}_k,\mathbf{Y}_k)\right] & E\left[-\Delta_{\mathbf{X}_{k-1}}^{\mathbf{x}_k}\log p(\mathbf{X}_k,\mathbf{Y}_k)\right] \\ E\left[-\Delta_{\mathbf{x}_k}^{\mathbf{X}_{k-1}}\log p(\mathbf{X}_k,\mathbf{Y}_k)\right] & E\left[-\Delta_{\mathbf{x}_k}^{\mathbf{x}_k}\log p(\mathbf{X}_k,\mathbf{Y}_k)\right] \end{bmatrix} \tag{2.21}$$

where $\Delta_x^y = \nabla_x\nabla_y^T$ and $\nabla_x = [\frac{\partial}{\partial x_1}, \cdots, \frac{\partial}{\partial x_n}]^T$. The recursive expression for $J(\mathbf{x_k})$ is derived in [17]. We denote $J(\mathbf{x_k})$ as J_k for brevity. The expression for J_k is given by

$$J_k = D_{k-1}^{22} - D_{k-1}^{21}(J_{k-1} + D_{k-1}^{11})^{-1}D_{k-1}^{12} \tag{2.22}$$

where,

$$\begin{aligned}
D_k^{11} &= -E\left\{\nabla_{\mathbf{x}_k}\left[\nabla_{\mathbf{x}_k}\log p(\mathbf{x}_{k+1}|\mathbf{x}_k)\right]^T\right\} \\
D_k^{21} &= -E\left\{\nabla_{\mathbf{x}_k}\left[\nabla_{\mathbf{x}_{k+1}}\log p(\mathbf{x}_{k+1}|\mathbf{x}_k)\right]^T\right\} \\
D_k^{12} &= (D_k^{21})^T \\
D_k^{22} &= -E\left\{\nabla_{\mathbf{x}_{k+1}}\left[\nabla_{\mathbf{x}_{k+1}}\log p(\mathbf{x}_{k+1}|\mathbf{x}_k)\right]^T\right\} \\
&\quad - E\left\{\nabla_{\mathbf{x}_{k+1}}\left[\nabla_{\mathbf{x}_{k+1}}\log p(\mathbf{y}_{k+1}|\mathbf{x}_{k+1})\right]^T\right\},
\end{aligned}$$

with J_0 computed from the initial density $p(x_0)$ as $J_0 = E\left\{[\nabla_{\mathbf{x}_0}\log p(\mathbf{x}_0)][\nabla_{\mathbf{x}_0}\log p(\mathbf{x}_0)]^T\right\}$. If the initial distribution is Gaussian: $\mathbf{x}_0 \sim \mathcal{N}(\mathbf{x}_0;\bar{\mathbf{x}}_0, P_0)$, then it is easy to show

that $J_0 = P_0^{-1}$. For a linear process model (1.3) and additive Gaussian noise with zero mean ((2.12), (2.13)) we have,

$$D_k^{11} = F^T Q_k^{-1} F \tag{2.23}$$
$$D_k^{12} = -F^T Q_k^{-1} \tag{2.24}$$
$$D_k^{22} = Q_k^{-1} + H_{k+1}^T R_{k+1}^{-1} H_{k+1} \tag{2.25}$$

where R_k is the measurement noise intensity matrix (see (2.13)) and $H_k = \left[\nabla_{\mathbf{x}_k} h^T(\mathbf{x}_k)\right]^T$ is the Jacobian of $h(\mathbf{x}_k)$ evaluated at the true state $\mathbf{x}_k$, related to the local terrain gradient represented by H_k^T. Thus, J_k can be written as

$$\begin{aligned} J_k &= Q_{k-1}^{-1} + H_k^T R_k^{-1} H_k \\ &\quad - \left(F^T Q_{k-1}^{-1}\right)^T \left(J_{k-1} + F^T Q_{k-1}^{-1} F\right)^{-1} F^T Q_{k-1}^{-1}. \end{aligned} \tag{2.26}$$

H_k for cooperative TAN with n vehicles is given by

$$H_k = \begin{bmatrix} H_{1_k} \\ H_{2_k} \\ H_{3_k} \end{bmatrix} = \begin{bmatrix} \frac{\partial h_1(\mathbf{x}_k)}{\partial x_k^1} & \frac{\partial h_1(\mathbf{x}_k)}{\partial y_k^1} & \cdots & \frac{\partial h_1(\mathbf{x}_k)}{\partial x_k^n} & \frac{\partial h_1(\mathbf{x}_k)}{\partial y_k^n} \\ \frac{\partial h_2(\mathbf{x}_k)}{\partial x_k^1} & \frac{\partial h_2(\mathbf{x}_k)}{\partial y_k^1} & \cdots & \frac{\partial h_2(\mathbf{x}_k)}{\partial x_k^n} & \frac{\partial h_2(\mathbf{x}_k)}{\partial y_k^n} \\ \frac{\partial h_3(\mathbf{x}_k)}{\partial x_k^1} & \frac{\partial h_3(\mathbf{x}_k)}{\partial y_k^1} & \cdots & \frac{\partial h_3(\mathbf{x}_k)}{\partial x_k^n} & \frac{\partial h_3(\mathbf{x}_k)}{\partial y_k^n} \end{bmatrix}.$$

H_k matrix represents the components of the local gradient of the terrain represented in the map with respect to the 2D coordinates. It is hard to attach some physical meaning to the terrain gradient at position of vehicle 2 with respect to the postion of the vehicle 1. Following common practice, in our simulations we consider that the derivative represented in the last row of the matrix are zero.
Notice that in the case of oportunistic coopertaive tan problem the states are only the positions of AUV1. The terrain gradient at the positions of AUV2 does not depends on the states (Postion of AUV1). In this case the altitude measurement of AUV2 will not contribute to the CRLB computation. The other possible solution lies in hypothetically assuming that the positions of AUV2 is also part of the states .Thus, the state vetcor can be written as $\mathbf{x}_k = [x_k^1,\, y_k^1,\, x_k^2,\, y_k^2]^T$ and H_k is given by

$$H_k = \begin{bmatrix} H_{1_k} \\ H_{2_k} \\ H_{3_k} \end{bmatrix} = \begin{bmatrix} \frac{\partial h_1(\mathbf{x}_k)}{\partial x_k^1} & \frac{\partial h_1(\mathbf{x}_k)}{\partial y_k^1} & 0 & 0 \\ \frac{\partial h_2(\mathbf{x}_k)}{\partial x_k^1} & \frac{\partial h_2(\mathbf{x}_k)}{\partial y_k^1} & \frac{\partial h_2(\mathbf{x}_k)}{\partial x_k^2} & \frac{\partial h_2(\mathbf{x}_k)}{\partial y_k^2} \\ 0 & 0 & \frac{\partial h_3(\mathbf{x}_k)}{\partial x_k^2} & \frac{\partial h_3(\mathbf{x}_k)}{\partial y_k^2} \end{bmatrix}.$$

However, the choice of process noise for AUV2 is still an issue. As the two vehicles chosen for the experiment were identical, we choose the same process noise as vehicle to be close to reality. The numerical computations of CRLB for CTAN and TAN only case are shown in figure 2.11

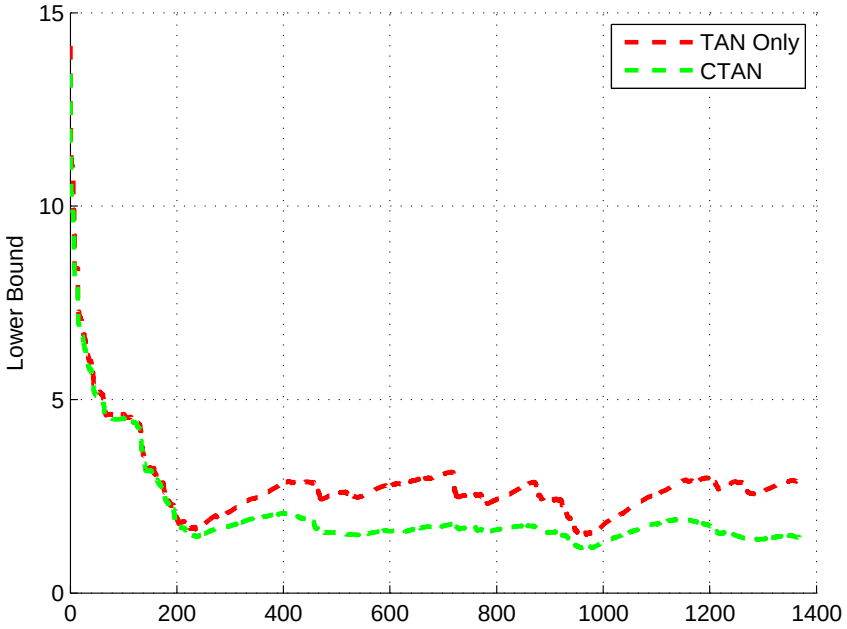

Figure 2.11: CRLB for cooperative TAN and TAN only case .

The inverse of matrix R_k is given by

$$R_k^{-1} = \begin{bmatrix} \frac{1}{\sigma_{1_k}^2} & 0 & 0 \\ 0 & \frac{1}{\sigma_{2_k}^2} & 0 \\ 0 & 0 & \frac{1}{\sigma_{3_k}^2} \end{bmatrix},$$

where $\sigma_{1_k}^2$ and $\sigma_{3_k}^2$ are the intensity of the sonar measurement noise for vehicle 1 and 2, and $\sigma_{2_k}^2$ is the intensity of the error η_{2_k} in the range measurements.

The Fisher information matrix represents the information content that can be extracted from the measurements with this particular system. In essence, this information is defined by the gradients of the measurement. Close examination of (2.26) also reveals that the FIM mainly depends on the term $S_k = H_k^T R_k^{-1} H_k$. If the gradient H_k^T undergoes discontinuities or if the local slope of the terrain is very large, S_k will change sharply, resulting in abrupt changes of J_k. This shows that the FIM is sensitive to local gradients and it is said to have the property of *locality* (see [18]). Notice that in case of terrain-based navigation the gradient of the measurement function corresponds to the gradient of the terrain represented in the map. As such, there are undesirable effects in terms of filter efficiency that can arise by using a map with high spatial variability induced by noisy measure-

ments if such noise is not properly modeled by the corresponding error model. This topic will be revisited in the next section. For TAN/SBN, the matrix S_k can be decomposed into a sum given by

$$S_k = S_{k_{TAN}} + S_{k_{CTAN}} \tag{2.27}$$

where

$$S_{k_{TAN}} = \frac{1}{\sigma^2_{1_k}} \left[\nabla_{\mathbf{x}_k} h_1^T(\mathbf{x}_k)\right] \left[\nabla_{\mathbf{x}_k} h_1^T(\mathbf{x}_k)\right]^T = \frac{1}{\sigma^2_{1_k}} H^T_{1_k} H_{1_k} \tag{2.28}$$

and

$$S_{k_{CTAN}} = H^T_{k_{CTAN}} R^{-1}_{k_{CTAN}} H_{k_{CTAN}}. \tag{2.29}$$

where,

$$H_{k_{CTAN}} = \begin{bmatrix} H_{1_k} \\ H_{2_k} \end{bmatrix} \quad \text{and,} \quad R^{-1}_{k_{CTAN}} = \begin{bmatrix} \frac{1}{\sigma^2_{2_k}} & 0 \\ 0 & \frac{1}{\sigma^2_{3_k}} \end{bmatrix}.$$

In (2.28) and (2.29), $\text{tr}(S_{k_{TAN}}) \geq 0$ and $\text{tr}(S_{k_{CTAN}}) \geq 0$. Thus, it can be concluded that

$$\text{tr}(S_k) \geq \text{tr}(S_{k_{TAN}}) \text{ and } \text{tr}(S_k) \geq \text{tr}(S_{k_{CTAN}}) \tag{2.30}$$

The expression for S_k above is used to compute J_k, from which the CRLB matrix follows by inverting it. The minimum covariance of the estimation error for $\mathbf{X}_k$ that can be obtained with any unbiased estimator is embodied in J_k and therefore in the CRLB matrix J_k^{-1}. Stated in simple terms, the larger the trace of J_k, the smaller the covariance is. Equation (2.30) shows that the trace of J_k will always be greater cooperative TAN than in the case of TAN only navigation only, thus showing clearly the advantage of using cooperative TAN. Actually, it can be shown from the above that adding new independent measurements characterized by non-zero gradients will contribute to reducing the CRLB further. As such, complementing TAN with mwasurements from another vehicle provides complementary information from two independent sources and allows for a reduction of the CRLB. Using computations similar to those presented above we can show that adding another vehicle will increase the information further for estimating the states. However, the combination of two vehicle will not provide a solution if both the vehicles are on the flat terrain. In the work reported here, the expression for J_k was instrumental in assessing the efficacy of TAN, and cooperative TAN and drawing comparisons among them. However, the importance of having such an expression goes well beyond the theoretical results that clearly show the advantage of complementing TAN with SBN. In fact, it affords a system designer the information required to evaluate the navigational performance that can be achieved as a function of the trajectories planned for an AUV, the type of terrain encountered, and the trajectories of other vehicles.

Bibliography

[1] Deborah Meduna. Terrain relative navigation for sensor-limited systems with application to underwater vehicles. Phd, Stanford University, 08/2011 2011.

[2] Francisco Curado Teixeira, João Quintas, and António Pascoal. Auv terrain-aided doppler navigation using complementary filtering. In *Proceedings of MCMC2012*, 2012.

[3] Francisco José Curado Mendes Teixeira, Pramod Maurya, and António Pascoal. A novel particle filter formulation with application to terrain-aided navigation. In *Proceedings of NGCUV2012*, 2012.

[4] Shandor Dektor and Stephen M. Rock. Improving robustness of terrain-relative navigation for auvs in regions with flat terrain. In *IEEE AUV 2012*, Southampton, England, 09/2012 2012.

[5] Alexander Bahr. *Cooperative Localization for Autonomous Underwater Vehicles*. PhD thesis, 2008.

[6] Hua Mu, T. Bailey, P. Thompson, and H. Durrant-Whyte. Decentralised solutions to the cooperative multi-platform navigation problem. *Aerospace and Electronic Systems, IEEE Transactions on*, 47(2):1433 –1449, april 2011.

[7] S. Webster, L. Whitcomb, and R. Eustice. Preliminary results in decentralized estimation for single-beacon acoustic underwater navigation. In *Proceedings of Robotics: Science and Systems*, Zaragoza, Spain, June 2010.

[8] N. Trawny, S.I. Roumeliotis, and G.B. Giannakis. Cooperative multi-robot localization under communication constraints. In *Robotics and Automation, 2009. ICRA '09. IEEE International Conference on*, pages 4394 –4400, may 2009.

[9] Francisco José Curado Mendes Teixeira. *Terrain-Aided Navigation and Geophysical Navigation of Autonomous Underwater Vehicles*. PhD thesis, Instituto Superior Técnico, 2007.

[10] Francisco Curado Teixeira. *Terrain-Aided Navigation and Geophysical Navigation of Autonomous Underwater Vehicles.* PhD thesis, Instituto Superior Técnico. DEEC, 2007.

[11] Fredrik Gustafsson, Fredrik Gunnarsson, Niclas Bergman, and Urban Forssell. Particle filters for positioning, navigation and tracking. *IEEE Transactions on Signal Processing*, (Special issue on Monte Carlo methods for statistical signal processing), 2001.

[12] Amanda Prorok and Alcherio Martinoli. A reciprocal sampling algorithm for lightweight distributed multi-robot localization. In *IROS*, pages 3241–3247, 2011.

[13] Dieter Fox, Wolfram Burgard, Hannes Kruppa, and Sebastian Thrun. A probabilistic approach to collaborative multi-robot localization. *Autonomous Robots*, 8:325–344, 2000. 10.1023/A:1008937911390.

[14] Lingji Chen Pablo, Pablo O. Arambel, and Raman K. Mehra. Estimation under unknown correlation: Covariance intersection revisited. *IEEE Transactions on Automatic Control*, 2002:1879–1882, 2002.

[15] B. Bayat and P. Aguiar. Auv range-only localization and mapping: Observer design and experimental results. In *ECC'13 - European Control Conference, Zurich, Switzerland, Jul. 2013.* ECC'13 - European Control Conference, Zurich, Switzerland, Jul. 2013, 2013.

[16] Harry Van Trees. *Detection , Estimation , and Modulation Theory Part I*, volume 6. John Wiley & Sons, Inc, 2001.

[17] Petr Tichavsky, Carlos H. Muravchik, and Arye Nehorai. Posterior Cramér-Rao bounds for discrete-time nonlinear filtering. *IEEE Transactions on Signal Processing*, 46(5), 1998.

[18] B. Roy Frieden and Bernard H. Soffer. Lagrangians of physics and the game of Fisher-information transfer. *Physical Review E*, 52(3):2274–2286, 1995.